Renewable and Sustainable Energy Reviews 112 (2019) 263–279

Contents lists available at ScienceDirect

Renewable and Sustainable Energy Reviews

journal homepage: www.elsevier.com/locate/rser

Reducing variability in the cost of energy of ocean energy arrays

Mathew B.R. Topper[a,*], Vincenzo Nava[b,c], Adam J. Collin[d], David Bould[e], Francesco Ferri[f], Sterling S. Olson[g], Ann R. Dallman[g], Jesse D. Roberts[g], Pablo Ruiz-Minguela[b], Henry F. Jeffrey[e]

[a] Data Only Greater, Maynooth, Ireland
[b] Tecnalia Research and Innovation, Energy and Environment Division, Derio, Spain
[c] BCAM - Basque Centre for Applied Mathematics, Bilbao, Spain
[d] University of Campania "Luigi Vanvitelli", Aversa, CE, Italy
[e] Institute for Energy Systems, University of Edinburgh, Edinburgh, UK
[f] Department of Civil Engineering, Aalborg University, Aalborg, Denmark
[g] Sandia National Laboratories, Albuquerque, United States

ARTICLE INFO

Keywords:
Financial
Variability
Energy
Ocean
Wave
Tidal
Arrays

ABSTRACT

Variability in the predicted cost of energy of an ocean energy converter array is more substantial than for other forms of energy generation, due to the combined stochastic action of weather conditions and failures. If the variability is great enough, then this may influence future financial decisions. This paper provides the unique contribution of quantifying variability in the predicted cost of energy and introduces a framework for investigating reduction of variability through investment in components. Following review of existing methodologies for parametric analysis of ocean energy array design, the development of the DTOcean software tool is presented. DTOcean can quantify variability by simulating the design, deployment and operation of arrays with higher complexity than previous models, designing sub-systems at component level. A case study of a theoretical floating wave energy converter array is used to demonstrate that the variability in levelised cost of energy (LCOE) can be greatest for the smallest arrays and that investment in improved component reliability can reduce both the variability and most likely value of LCOE. A hypothetical study of improved electrical cables and connectors shows reductions in LCOE up to 2.51% and reductions in the variability of LCOE of over 50%; these minima occur for different combinations of components.

1. Introduction

The design of an ocean energy array is highly complex and exhibits many possible solutions. Although early demonstrator projects and arrays have been successfully deployed (see e.g. [1–3]) there has yet to emerge a standard design process for ocean energy arrays. This is likely, in part, due to the early technology readiness level of the industry and the broad range of technologies that are available ([4,5]). Assuming that the internal design of the deployed ocean energy converter (OEC) is fixed, the design of an OEC array can be divided into the following general stages:

- Selecting the location of the OECs and calculating the energy produced;
- Designing the transmission network for the electricity generated by the OECs;
- Designing the station keeping requirements of the OECs in the chosen locations;
- Planning the installation of the OECs and array infrastructure;
- Planning the maintenance of the OECs over the lifetime of the array and recording any energy lost due to failure;
- Planning the removal (decommissioning) of the array following the end of its useful life.

Many studies exist which cover the individual stages of the OEC array design process. The optimal positioning of wave and tidal converters in an array has been discussed by [6,7], for example. Software tools also exist for helping designers optimise the location of OECs, such as WaveFarmer [8], TidalFarmer [9], and to evaluate and minimize the array's potential environmental impact (e.g. SNL-SWAN [10] and SNL-

* Corresponding author.
E-mail addresses: mathew.topper@dataonlygreater.com (M.B.R. Topper), vincenzo.nava@tecnalia.com (V. Nava), adam.collin@ieee.org (A.J. Collin), david.bould@ore.catapult.org.uk (D. Bould), ff@civil.aau.dk (F. Ferri), ssolson@sandia.gov (S.S. Olson), ardallm@sandia.gov (A.R. Dallman), jdrober@sandia.gov (J.D. Roberts), jpablo.ruiz-minguela@tecnalia.com (P. Ruiz-Minguela), Henry.Jeffrey@ed.ac.uk (H.F. Jeffrey).

https://doi.org/10.1016/j.rser.2019.05.032
Received 23 July 2018; Received in revised form 4 May 2019; Accepted 13 May 2019

List of abbreviations, units and nomenclature

C	CAPEX for N years
E	AEP for N years
O	OPEX for N years
P	power output of OECs within year m
C_{op}	total cost of a logistics operation
E_m	AEP for year m
H_{m0}	significant wave height
M	metocean time series data
N	number of years in which the array is operational
O_m	OPEX for year m
T	time of sub-system failure
T_e	wave energy period
T_m	planned production time in year m
T_{op}	total duration of a logistics operation
T_{pause}	sum of t_{pause} for all operations
c_i	cost of ith 11kV static cable
c_j	cost of jth 11kV wet-mate connector
d	discount rate
n_{op}	number of operations in year m
r_{access}	cost rate over t_{access}
r_{action}	cost rate over t_{action}
r_{delay}	cost rate over t_{delay}
r_{pause}	cost rate over t_{pause}
r_{prep}	cost rate over t_{prep}
r_{return}	cost rate over t_{return}
r_{wait}	cost rate over t_{wait}
t_{access}	time required to access the target of the logistics action
t_{action}	duration of a logistics action
t_{delay}	time between logistics action request and commencing the action
t_{pause}	sum of durations between weather windows
t_{prep}	logistics action preparation time
t_{return}	time to return following a logistics action
t_{wait}	time until a weather window is available
η	electrical network efficiency
λ	sub-system failure rate
τ_{depart}	earliest logistics operation departure date
τ_{start}	logistics action request date
θ_i	MTTF of ith 11kV static cable
θ_j	MTTF of jth 11kV wet-mate connector
AEP	annual energy production
CAPEX	capital expenditure
HPP	homogeneous Poisson process
KDE	kernel density estimator
LCOE	levelised cost of energy
MTTF	sub-system mean time to failure
NPV	net present value
OEC	ocean energy converter
OLCs	operational limit conditions
OPEX	operational expenditure
PDF	probability density function
RM3	Reference Model 3

Delft3D-CEC [11]). Studies have been undertaken to automate the design of the electrical network ([12,13]) and regarding choices for OEC station keeping ([14,15]). Optimisation of installation of OECs using the commercial planning software 'Mermaid' is presented in [16] and other recent studies, such as [17,18], have considered the cost of maintenance activities required for arrays of wave energy converters.

Automatic integrated design of arrays has the potential to bring significant benefits to the ocean energy industry, as has been demonstrated for offshore wind energy [19]. Unfortunately, effective communication of specifications between design stages can be difficult to achieve. Semantic conflicts and change management issues, known as *semantic heterogeneity* [20], make developing software to facilitate interoperability extremely challenging.

Some integrated design approaches have been attempted for ocean energy array design. An integrated approach to calculating the costs of an array of floating tidal turbines is addressed in [21]. The Reference Model project [22] demonstrated a hybrid analytical and computational approach to the entire ocean energy array design process and another hybrid approach for co-located wind and wave energy is presented in [23]. In [24] the positions of an array of wave energy converters are optimised by combining precise power production calculations and a basic empirical cost model within a genetic algorithm. The method described in [25] used a computational approach for evaluating the impact of OEC design and site selection on the maintenance operations required throughout the lifetime of the array.

The existing approaches do not consider all stages of ocean energy array design as parametric, nor allow automated assessment of modifications at component level. Yet, understanding how individual components, or groups of components, impact the costs of ocean energy arrays is critical for improving the readiness level of ocean energy technologies [26]. Comparison of energy generation technologies is often achieved using cost of energy metrics. The ratio of the lifetime costs of an array to the energy generated is the most basic formula. This can be improved by considering discounting of future costs, as shown in [27], to produce the levelised cost of energy (LCOE) metric. When considering the cost of energy, it may be that a range of possible values exist, which can be attributed to *uncertainty* and *variability*. These concepts can be described following the definitions in [28]:

Uncertainty derives from a lack of knowledge. A parameter is uncertain if the range of values it can take can be reduced by gaining more or better quality data.

Variability is a characteristic of data that is naturally stochastic. Variability of a parameter cannot be reduced, but understanding of the variability can be improved through increased sampling.

How uncertainty in failure rates affects the maintenance requirements of deployments of the Pelamis P2 OEC is studied in [18]. Following the approach of [29], a sensitivity analysis is undertaken to quantify uncertainty in the final productivity and cost outcomes. Pure economic analyses will also address uncertainty of inputs by considering a range of values for both costs and energy production (e.g. [30]).

The assumption in these studies is that if the inputs were better understood, the results would become purely deterministic. The present work provides the unique contribution of demonstrating that predicted ocean energy costs will always exhibit variability, due to the significant influence of variable weather conditions combined with random component failures. It also hypothesises that if the variability is found to be substantial then it may play an important role in investment decisions. The work quantifies variability resulting from maintenance actions although other sources of variability are present, such as in the power generation and installation operations, that are not specifically addressed here. By developing a framework for modelling investment in components to improve reliability, it will be shown that the cost of energy and its variability can be reduced.

This goal is realised using an integrated, parametric model of ocean energy array design with higher complexity than seen before. In particular, sub-systems are designed at component level which combine to give the sub-system reliability. Thus, the impact of individual component choices can be analysed over the lifetime of the array.

The software implementation of the model presented herein, named DTOcean, was originally released to the public following conclusion of the European Commission funded Optimal Design Tools for Ocean

Energy Arrays (DTOcean) project [31] under an open source licence (available from www.github.com/DTOcean). Since then, the underpinning theory and software have been continually developed and, at the time of writing, represents one of the most advanced comprehensive tools for the conceptual design of ocean energy arrays. The software continues development as part of the Advanced Design Tools for Ocean Energy Systems Innovation, Development and Deployment (DTOcean-Plus) project [32] which will add support for the entire ocean energy development process, from the selection and development of sub-systems and energy capture devices to full array deployment.

The outline of the work is as follows. Section 2 presents the key elements of the array design software, measurement of cost variability and component investment framework. In section 3, a case study is used to demonstrate the theory and establish a base case for investigating the impact of component changes. Section 4 discusses the results while conclusions are drawn in the final section.

2. Method

2.1. Software overview

The DTOcean software simulates, combines and assesses the design stages described in section 1, apart from decommissioning which, similarly to [22], was deemed to have negligible impact on LCOE. At the time of writing, the software can be used for simulations of OEC array deployments falling within the scope and subject to the assumptions shown in Table 1.

A schematic showing the relationships between the key software elements and the user is shown in Fig. 1. Each of the five simulated design stages is calculated by a distinct module, collectively referred to as 'design modules', which are configured to the project requirements. A design module may also utilise the functionality of other modules, known as 'support modules'. Design or support modules may seek a locally optimal result appropriate to the modules' purpose. The 'assessment modules' combine outputs into metrics useful to the design modules or for comparison of simulations. The purpose and optimisation strategy (if applicable) for the design, support and assessment modules are shown in Table 2. As the environmental impact assessment within DTOcean has no influence on the predicted costs of the array, it is not considered within this study.

Data transfer between the software elements is managed by the 'Core' module, in which a 'common data model' [33] is defined to facilitate interoperability between the five design stages, and provide a digital representation of the array. The logical connections between modules are determined by data transfer; Fig. 2 shows the most pertinent outputs of each module and the transfer of outputs between modules. Only a subset of the total number of variables is shown in Fig. 2 and DTOcean's high level of complexity is illustrated by the number of variables contained in the data model, having approximately 550 at the time of writing. Further details of the module implementations and data model design are available from [34].

Table 1
Simulation scope and modelling assumptions of the DTOcean software.

OEC types	Floating or bottom fixed; wave or tidal
Mixed OEC types	Single type per simulation
Maximum number of OECs	100
Maximum deployment depths	80m for tidal, 200m for wave
Sedimentary layers	Single or multi-layered strata
Electrical network types	Single substation, single export cable
Foundation types	Gravity, piles, anchors, suction caissons, shallow
Mooring types	Catenary or taut
Logistics	Single port, one vessel per operation
Maintenance strategies	Corrective, calendar or condition based

2.2. Inputs

The DTOcean software is designed for analysing deployments of multiple wave or tidal energy converters, typically at the planning stage following project licensing. Assuming compliance with contemporary standards (such as [35–37]), the users are anticipated to have a comprehensive dataset from which to design an array, including geographical, geological and OEC design data. The DTOcean tool seeks to fully utilise datasets of this magnitude, and some key inputs are detailed below. Example datasets, including the case study presented herein, are stored within the database distributed alongside the software.

2.2.1. Geography and geology

The topography of a DTOcean project is defined using two domains, the 'deployment area', in which the OECs should be placed, and the 'cable corridor', which bounds the path of the export cable. Both domains share certain data requirements such as:

- Layers of seabed sediment; multiple layers can be defined, chosen from various grades of sand, clay and rock;
- A single representative time series of wind and current magnitudes, wave heights and wave periods;
- Optional 'no-go areas', where the software may not place OECs or infrastructure.

Within the deployment area, additional data are required, including:

- For tidal energy converter simulations, a time series of velocity, sea level and turbulence intensity over the entire deployment area;
- Wave energy converter simulations require a single time series, representative of the deployment area, containing wave height, wave period and mean direction;
- Representative, extreme conditions for wind, wave and currents.

2.2.2. Ocean energy converter

It is required that each deployment will use only a single OEC type and that its characteristics are known prior to commencing the simulation (i.e. no OEC modifications are made as part of the simulation process). The inputs include:

- Various OEC dimensions such as the location of foundations and mooring connection points, as applicable;
- Power performance data, requiring thrust/power curves for tidal OECs and power matrices for wave OECs;
- Electrical specifications, such as operating voltage and connector types.

The OEC sub-systems are divided into the support structure, prime mover and power take-off for simulating installation and maintenance (an optional control system can be added, but is not used here). Each sub-system requires data such as costs, failure rates and operational parameters.

2.3. Layout and energy production

Understanding of the key influences on the final LCOE of an ocean energy converter array is greatly enhanced when the positioning of the major components can be controlled.

Positioning OECs relative to the local environment and other OECs allows the power production to be optimised subject to array interactions and site constraints. The hydrodynamics module of DTOcean seeks the optimal positions by applying a Covariance Matrix Adaptation Evolution Strategy to the power produced from a parameterised array structure [38]. The strategy is constrained by a minimum threshold for the 'q-factor'. The q-factor is the ratio of the power absorbed by the

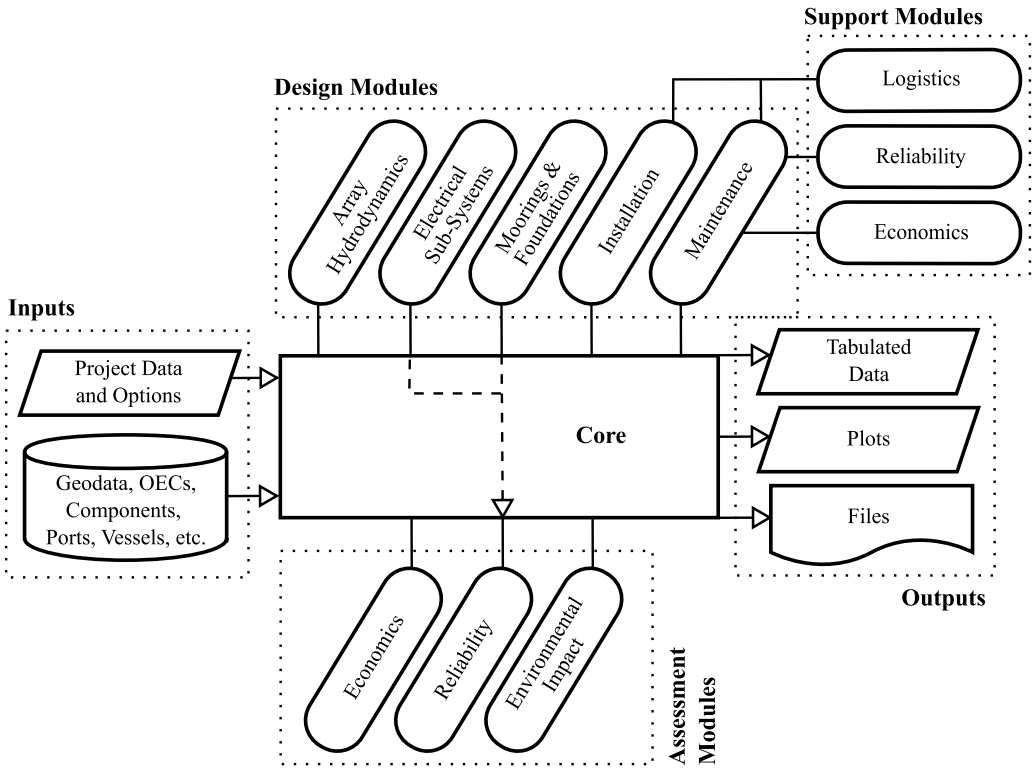

Fig. 1. Relationships between the key software elements and user. Data is transferred between the user, database, design and assessment modules by the core. The core also sequences the execution of modules. Support modules provide functionality shared between multiple design or assessment modules, and are accessed directly. Specific data transferred between modules is shown in Fig. 2.

OECs with and without interference. An array containing a single OEC would have a q-factor of unity, for example.

For wave energy converters, the calculation of the power absorbed and OEC interactions utilises the open-source boundary element method software NEMOH [39] combined with the direct matrix method approach presented in [40]. For tidal energy converters, an actuator disc model is combined with the wake interaction method described in [41], which is further enhanced by replacing the wake decay model with a dataset of computational fluid dynamics simulations. Additionally, the wake velocity deficits are calculated relative to the streamlines of the turbine rather than assuming that the wake is straight. Once the power per sea state is known for each device, energy production can be calculated by combination with metocean data.

Cables and substations for the electrical network are intelligently sited using the DTOcean electrical sub-systems module. Each array must include one substation and a single export cable from the substation to the cable landing point. The OECs are then connected to the substation by a number of shared strings. Prior to populating the network and calculating its efficiency, various cable routes are generated, using a planar open vehicle routing algorithm developed for cable layout in offshore wind farms [42]. If the OEC is floating, an initial estimate at the required umbilical cable length and its point of connection to the network is also calculated, which is finalised when the moorings design is completed.

The selection of appropriate foundations for an ocean energy converter is important to establishing accurate lifetime costs associated to station keeping. Through knowledge of the OEC position, relative foundation locations and seabed sediment the DTOcean moorings and foundations module can discard foundation types which are not appropriate for the given sediment type. The remaining foundation types are then assessed for economic performance.

2.4. Component selection and reliability

DTOcean includes an extensive repository of technical data for components which can be used in the electrical sub-systems and moorings and foundations designs (see e.g. [43]). These data include estimates for the reliability of the components, as is discussed in [44], and costs.

The electrical sub-systems module selects a set of components to transmit the energy generated by the array to shore. Once the OEC power outputs are calculated, a set of suitably rated components is chosen. The Python package PYPOWER [45,46] is then used to calculate the power flow and associated power losses from all potential cable route combinations. The solution with least cost per electrical unit transmitted is returned.

The moorings and foundations module uses the available components to create a design capable of withstanding the long term extreme environmental conditions, subject to the OEC position and the local geology. Maximum loads, moments and displacements are calculated from static and quasi-static analysis within an iterative procedure to find a mooring and foundation design in equilibrium with the calculated forces [47]. The module selects the lowest cost set of components from the feasible solutions.

The components selected for the electrical and moorings and foundations designs are structured into networks which record the connectivity between sub-systems and the components within them; connections can be in series or parallel. Supplementary data associated to the nodes of the network are also generated, such as the lengths of cable segments. The networks are used to calculate reliability metrics for sub-systems and the entire array. The DTOcean reliability module combines failure rates of components using varying analytical expressions depending on the connectivity. A reliability indicator between

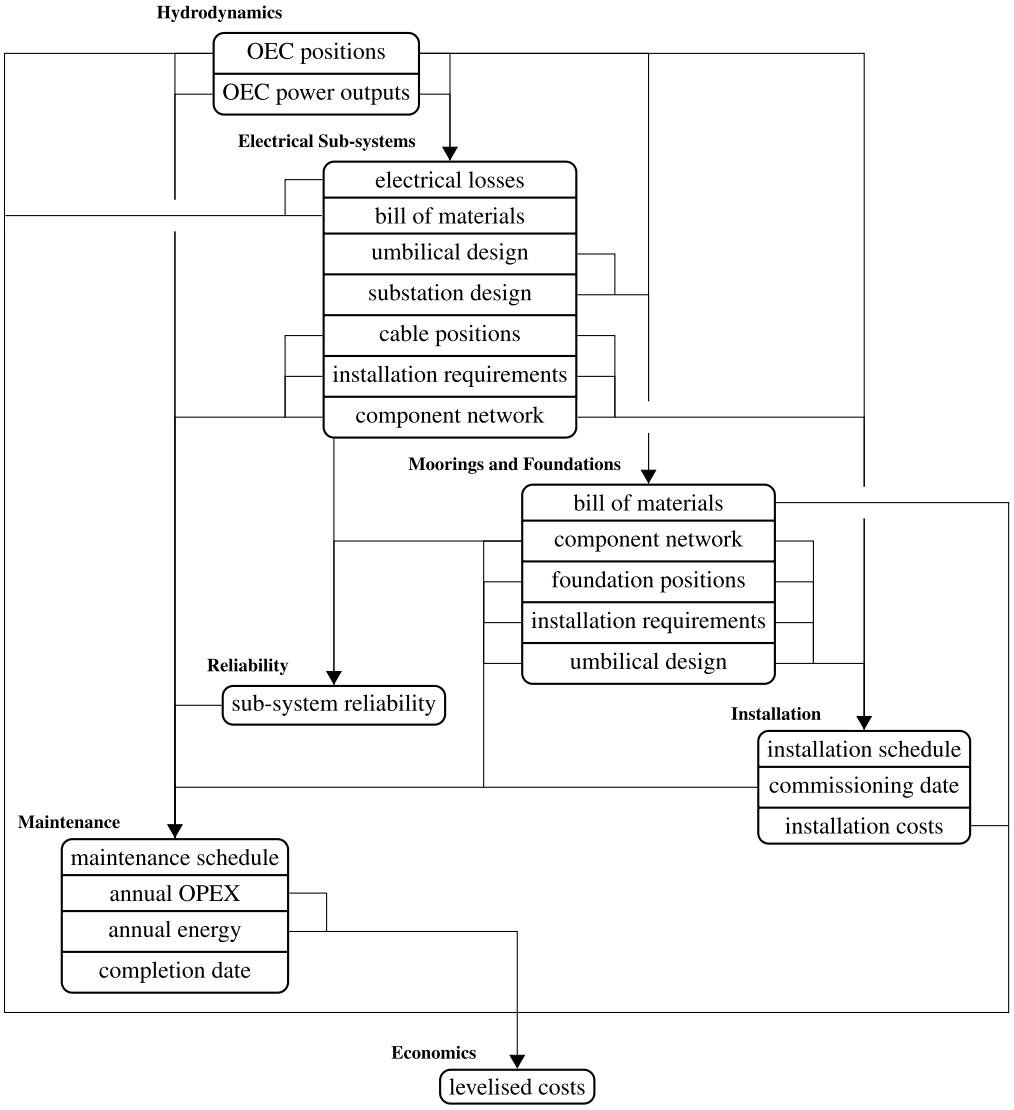

Fig. 2. Pertinent output data and its transfer between modules. Nodes represent modules, output parameters are shown in node cells and lines show exchange of parameters between modules (paths travel down or across).

Table 2
Description of modules provided by the DTOcean software.

Name	Category	Purpose	Local Optimisation Strategy
Array Hydrodynamics	Design	Locate OECs and calculate their power generation per sea state	OECs positioned for maximum power output
Electrical Sub-Systems	Design	Design electrical network suited to the OEC and export cable characteristics and calculate losses	Minimise cost per unit energy
Moorings and Foundations	Design	Design foundations and moorings (if appropriate) subject to array requirements and extreme conditions	Minimise cost
Logistics	Support	Calculate vessel and equipment requirements, costs and durations for installation or maintenance phases	Minimise cost within a maximum time limit
Installation	Design	Schedule the installation of all requested design phases	Minimise cost within a maximum time limit per phase
Reliability	Support/ Assessment	Combine components networks into reliability metrics for major sub-systems	Not applicable
Economics	Support/ Assessment	Calculate absolute or probabilistic costs for each design stage	Not applicable
Maintenance	Design	Schedule the maintenance activity over the array lifetime and record yearly costs and energy production	Minimise logistics cost subject to the maintenance strategy and maximum time limit
Environmental Impact	Assessment	Assess the environmental impact of the array design	Not applicable

zero and one for a given mission time or a mean time to failure (MTTF) of any component, sub-system or the entire array is given [48].

Sub-systems are described as either 'OEC-level' or 'array-level'. The OEC, inter-array cables, umbilical cable, moorings and foundations sub-systems are 'OEC-level'; the substation and export cable sub-systems are 'array-level'. Combining the reliability metrics for OEC-level sub-systems allows each OEC to have a unique set of failure modes and probabilities of failure. Incorporating the metrics of array-level sub-systems allows individual OEC, partial and full array failures to be simulated.

2.5. Logistics

The costs and durations of an installation or maintenance operation are calculated through detailed planning of its associated sub-tasks. The DTOcean logistics module selects appropriate vessels and equipment and calculates the time required to complete all sub-tasks subject to environmental conditions. From all feasible vessel and equipment combinations, the minimum cost solution is chosen, starting no later than a year after the operation request date. Seasonality and delays due to unfavourable conditions are captured, which has a direct impact on the cost variability discussed in this paper. In particular, the total cost and duration of an operation, C_{op} and T_{op}, are defined:

$$C_{op} = \begin{pmatrix} r_{delay} \\ r_{action} \\ r_{return} \end{pmatrix} \cdot \begin{pmatrix} t_{delay} \\ t_{action} \\ t_{return} \end{pmatrix} + C_{fixed}$$
$$T_{op} = t_{delay} + t_{action} + t_{return} \quad (1)$$

The delay time, t_{delay}, is the time between the action request date, τ_{start}, and beginning the physical action. t_{action} is the time required to carry out the physical action, such as a repair, and t_{return} is the time required to return to port, once the action is complete. r_{delay}, r_{action} and r_{return} are the associated cost rates and C_{fixed} refers to any fixed costs, such as spare parts.

Each sub-task, vessel and equipment have maximum allowable values for wind, waves and currents, called operational limit conditions (OLCs). Weather windows are time periods where environmental conditions less than the minimum OLCs are identified in metocean time series data (M). Subsequently, the delay time can be further subdivided as follows:

$$t_{delay} = t_{prep} + t_{access} + t_{wait} + t_{pause} \quad (2)$$

where t_{prep} is the preparation time, t_{access} is the time required to access the target of the logistics action, t_{wait} is the amount of waiting time until a weather window is available to commence the operation and t_{pause} is the summation of the durations between any subsequent windows required to complete the operation. Matching cost rates are also defined.

The earliest departure date for the operation, τ_{depart}, is given by:

$$\tau_{depart} = \tau_{start} + t_{prep} \quad (3)$$

Subsequently, the calculation of t_{wait} and t_{pause} can be expressed:

$$t_{wait} + t_{pause} = f(M, OLCs, \tau_{depart}) \quad (4)$$

The algorithm which describes the function f is given below.

To begin, the minimum of all OLCs in the operation's sub-tasks is taken and suitable weather windows are found in M. Assuming some weather windows exist, differing strategies are applied. The default strategy attempts to find windows which are long enough to encompass all sub-tasks of the operation, as follows:

1. Calculate the required window duration ($t_{\text{access}} + t_{\text{action}} + t_{\text{return}}$);
2. Iterate through each year of the time series data, searching for windows after τ_{depart};
3. Record t_{wait} of the first weather window with sufficient duration, within that year;
4. Return the mean t_{wait} over all years; t_{pause} is zero.

If no single weather window of suitable duration can be found (as is the often the case for long operations) then an alternative strategy is used:

1. Calculate the required window duration ($t_{\text{access}} + t_{\text{action}} + t_{\text{return}}$);
2. Iterate through each year of the time series data, searching for windows after τ_{depart};
3. Form groups from the ensuing weather windows such that the sum of the durations exceeds the total required;
4. Record t_{pause} for each group;
5. Find the group of windows with minimum t_{pause};
6. Record t_{wait} for the first window of the chosen group;
7. Return the mean t_{wait} and t_{pause} over all years.

It is assumed that $r_{\text{wait}} = 0$ and $r_{\text{pause}} = r_{\text{access}}$, thus the above strategy seeks to minimise cost but may incur large t_{wait}. An alternative is to minimise t_{wait} but suffer potentially costly increases in t_{pause}. Such a strategy is utilised for maintenance operations in the event of unplanned sub-system failures.

Further details of the remaining time and cost calculations, including the route-finding, and port, vessel and equipment selection algorithms, are available in [49]. In particular, drawing on the experience of the offshore wind industry, it is assumed that a single port is used for all operations and only one vessel (of any type) will be required per operation. All feasible port, vessel and equipment combinations for the operations are selected from the extensive database included in DTOcean.

2.6. Lifetime energy and costs

The operational phase of the array commences after a given commissioning period. The DTOcean maintenance module calculates the operational expenditure (OPEX) and energy production over the array lifetime by simulating failures and maintenance for sub-systems of the OEC, electrical network, moorings and foundations.

For each sub-system, a series of dates on which failures occur are generated using a homogeneous Poisson process (HPP), using the failure rate as the intensity parameter [48]. The probability of failure before time t is given by:

$$P(T \leq t) = 1 - \exp^{-\lambda t} \quad (5)$$

where T is the time of failure and λ is the failure rate. When a failure is detected, an 'unplanned corrective' maintenance operation is ordered. In this case, the shortest time to repair logistics strategy is used which may incur costly levels of t_{pause}. 'Downtime' is accrued from the point of failure of an OEC to the time of repair (equivalent to $t_{\text{delay}} + t_{\text{action}}$, in this case). This has the effect of stopping the energy production of the affected OEC(s) but also extending the time to the next failure date, simulating the additional life expected from the sub-system not being in operation.

A strategy of regular 'time-based' maintenance can also be chosen for any sub-system type. In this case, the model for probability of failure changes to assume such sub-systems exhibit perfect reliability prior to their given MTTF. Assuming MTTF = λ^{-1}, the probability of failure becomes:

$$P(T \leq t) = \begin{cases} 0 & t \leq MTTF \\ 1 - \exp^{-\lambda t} & t > MTTF \end{cases}$$

The interval for maintenance can be chosen as desired and each operation is undertaken using the minimum cost logistics strategy. Again, downtime will be accrued while the sub-system is undergoing maintenance, reducing the energy production.

To illustrate how random sub-system failures (captured by the HPP)

combine with environmental conditions to introduce variability into the levelised costs, consider, for any given year m, the array OPEX and annual energy production (AEP) in that year, written O_m and E_m respectively. Assuming all operations are unplanned (such that the downtime is always equal to $t_{\text{delay}} + t_{\text{action}}$),

$$O_m = \sum_{i=1}^{n_{op}} (C_{op})_i,\ E_m \approx \eta \left(T_m - \sum_{i=1}^{n_{op}} (t_{delay})_i + (t_{action})_i \right) P$$

Here, n_{op} refers to the number of operations in year m, η is the electrical network efficiency, T_m is the planned production time in year m and $\mathbf{P}$ is the power output of the OECs at any particular time within that year. C_{op} and t_{delay} are shown to be dependent on the metocean conditions, M, and the action request date, τ_{start}, by the combination of eqs. (1)–(4). Within the maintenance calculations, τ_{start} is determined by the random process governed by eq. (5), thus it can be inferred that, due to the temporal variability of metocean conditions, both O_m and E_m must also be treated in a probabilistic sense.

The LCOE equation is written:

$$LCOE = \frac{NPV(C) + NPV(O)}{NPV(E)} \tag{6}$$

where, **C** is the capital expenditure (CAPEX), **O** is the OPEX and **E** is AEP of the array, for the N years in which the array is operational. The net present value (NPV) is defined as:

$$NPV(x) = \sum_{m=0}^{N} \frac{x_m}{(1+d)^m}$$

where d is the discount rate. The CAPEX combines (principally) the installed cost of devices, and the electrical, moorings and foundation components, and is assumed deterministic.

The introduction of O_m and E_m into eq. (6), renders the LCOE equation probabilistic. A bivariate kernel density estimator [50] is applied to the OPEX and AEP terms in order to produce a bivariate probability density function (PDF). The maximum of the PDF can be used to determine the most likely combination of the OPEX and energy production and, thus, the LCOE. Additionally, by calculating the LCOE values along the 95th percentile contour of the bivariate PDF, the 95th percentile range of the LCOE can be found, which provides a standard metric for the variability.

2.7. Measuring the impact of investment

It is trivial to surmise that improved component reliability, without additional cost, will result in lower LCOE with reduced variability due to lower OPEX and less downtime. Establishing an acceptable level of capital investment in order to improve the reliability of components is a more nuanced question, particularly for complex sub-systems such as the inter-array cables which include multiple component types.

To investigate the use of more reliable, more expensive components, a general model for manufacturing costs is applied. Following [51], the production cost of a component, c, has a relationship to reliability of the form:

$$c(\theta) = A + B\theta^i \tag{7}$$

where θ is the reliability parameter (in this case MTTF), i is the order of the function and A, B are positive constants, to be determined.

It is important to assess whether changes in LCOE due to component changes are statistically significant from the base case. One technique to determine if arbitrary distributions differ from each other is by examining the energy distance between the distributions. The energy distance is a statistical distance between random vectors X, $Y \in R$ with cumulative distributions functions F and G, respectively [52]. The squared energy distance is defined:

$$D^2(F, G) = 2\mathbb{E}(||X - Y||) - \mathbb{E}(||X - X'||) - \mathbb{E}(||Y - Y'||) \geq 0$$

where X' and Y' are independent and identically distributed copies of X and Y, respectively, $||\cdot||$ is the euclidean norm and $\mathbb{E}$ denotes expected value. The null hypothesis that $F = G$ is true if and only if $D = 0$. From this result, a test statistic, T, is defined in [52] that when utilised with permutation tests gives an approximate p-value of the significance.

The ability to monitor change in LCOE and its variability as components are modified allows the optimal investment cost [53] to be established. The case study undertaken in the next section will provide a baseline measure of LCOE and variability for which investment in component upgrades can be investigated.

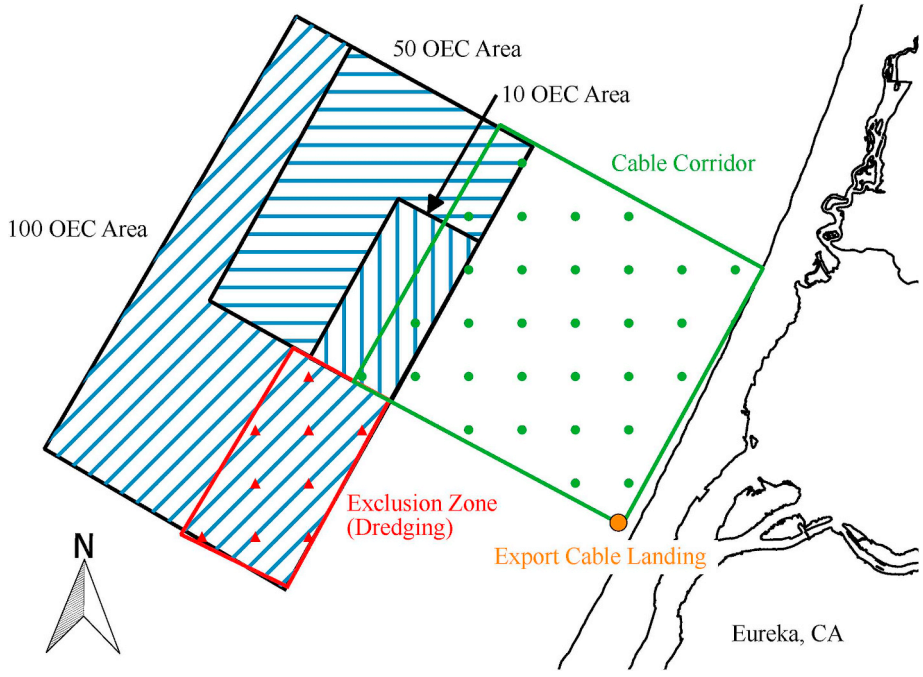

Fig. 3. Schematic map of the RM3 scenario deployment areas.

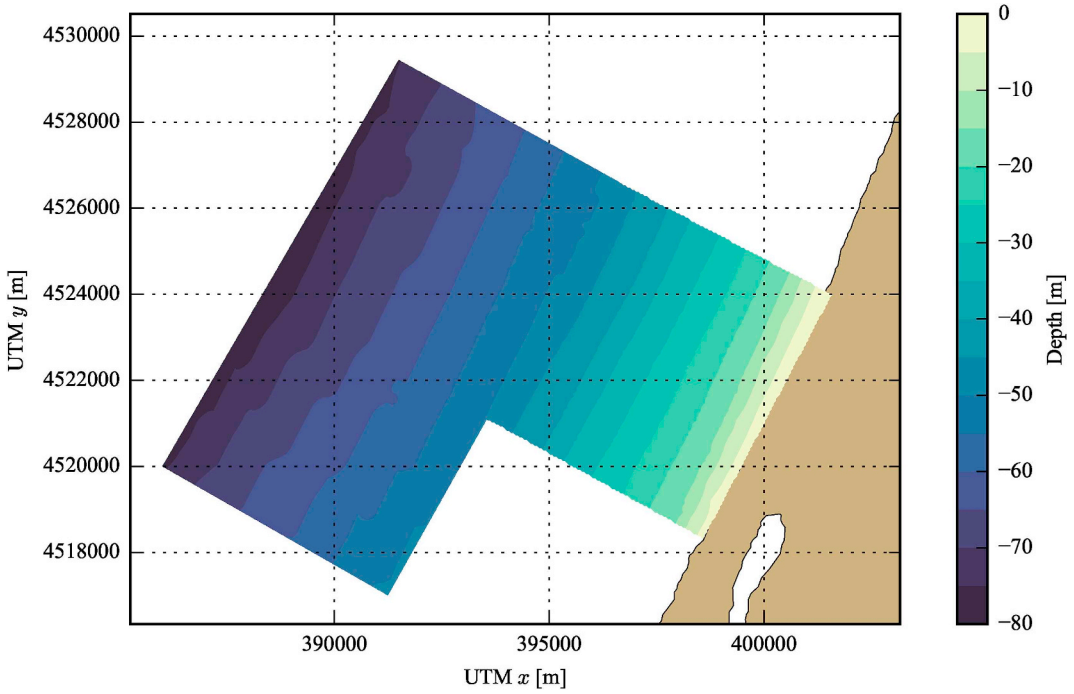

Fig. 4. Seabed depth at the RM3 site.

3. Case study

A case study of a floating wave energy converter array is presented. Wave energy extraction is likely to exhibit more variability than tidal energy, as ocean waves are less predictable than tides. Also, a floating OEC allows demonstration of the moorings and umbilical cable design features of DTOcean. The theoretical 'Reference Model 3' (RM3) array of floating point absorbers, as detailed in [22], matches the requirements above. The array is simulated at three scales of deployment (10, 50 and 100 OECs) and then an assessment of the impact of investment in more reliable components for the 10 OEC deployment is conducted.

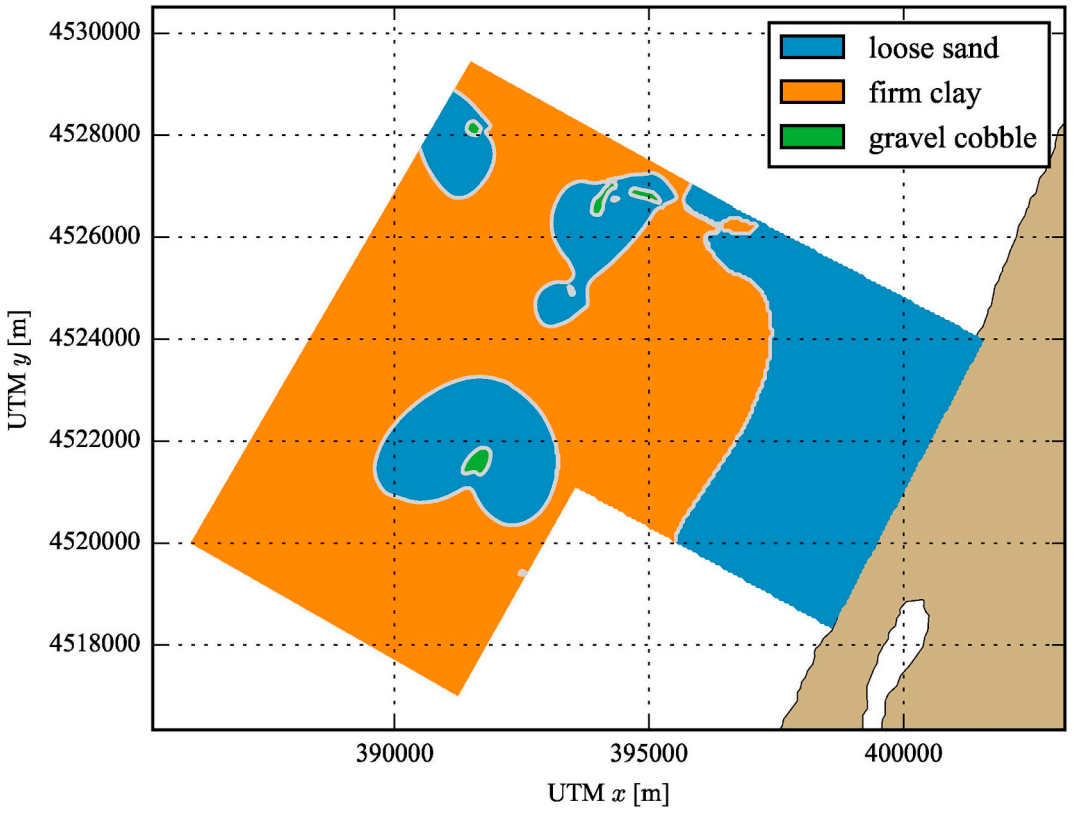

Fig. 5. Sediment types at the RM3 site.

H_{m0} [m] \ T_e [s]	4.5	5.5	6.5	7.5	8.5	9.5	10.5	11.5	12.5	13.5	14.5	15.5	16.5	17.5
0.25	0.00	0.00	0.00	0.01	0.03	0.00	0.00	0.00	0.00	0.00	0.00	0.00	0.00	0.00
0.75	0.02	0.35	1.41	2.16	1.20	0.63	0.14	0.05	0.01	0.01	0.00	0.00	0.00	0.00
1.25	0.02	1.69	4.16	5.26	3.46	1.98	0.85	0.40	0.14	0.04	0.02	0.00	0.00	0.00
1.75	0.00	0.89	6.11	4.84	4.84	3.46	1.82	1.01	0.55	0.27	0.02	0.00	0.00	0.00
2.25	0.00	0.00	3.43	4.20	3.61	4.26	2.88	1.55	0.80	0.61	0.14	0.02	0.01	0.00
2.75	0.00	0.00	0.18	1.70	1.66	3.18	3.03	1.82	0.89	0.42	0.20	0.05	0.01	0.01
3.25	0.00	0.00	0.00	0.09	0.49	1.62	2.30	1.54	0.92	0.41	0.16	0.06	0.03	0.01
3.75	0.00	0.00	0.00	0.00	0.07	0.74	1.54	1.33	0.55	0.31	0.16	0.05	0.02	0.00
4.25	0.00	0.00	0.00	0.00	0.01	0.12	0.70	0.81	0.44	0.24	0.12	0.05	0.01	0.00
4.75	0.00	0.00	0.00	0.00	0.00	0.02	0.21	0.41	0.35	0.13	0.08	0.02	0.01	0.00
5.25	0.00	0.00	0.00	0.00	0.00	0.01	0.06	0.20	0.22	0.11	0.07	0.00	0.00	0.00
5.75	0.00	0.00	0.00	0.00	0.00	0.00	0.02	0.08	0.16	0.09	0.03	0.00	0.00	0.00
6.25	0.00	0.00	0.00	0.00	0.00	0.00	0.00	0.02	0.07	0.03	0.05	0.00	0.00	0.00
6.75	0.00	0.00	0.00	0.00	0.00	0.00	0.00	0.00	0.03	0.03	0.02	0.00	0.00	0.00
7.25	0.00	0.00	0.00	0.00	0.00	0.00	0.00	0.00	0.02	0.01	0.01	0.00	0.00	0.00
7.75	0.00	0.00	0.00	0.00	0.00	0.00	0.00	0.00	0.00	0.01	0.00	0.00	0.00	0.00
8.25	0.00	0.00	0.00	0.00	0.00	0.00	0.00	0.00	0.00	0.01	0.00	0.00	0.00	0.00

Fig. 6. Wave occurrence matrix at the RM3 site (%).

3.1. Inputs

3.1.1. Geography and geology

The RM3 scenario considered an offshore, moderate depth site on the west coast of the United States of America near Eureka, in Humbolt County, California. Local infrastructure exists to support installation, operation, and maintenance of the array, with a 60kV substation available near Eureka and a deep-water port within Humbolt Bay.

Depths compatible with the selected OEC are found between 5 and 15km offshore, whilst the available deployment area extends for approximately 60km along the shoreline. The cable corridor was arbitrarily defined from the shoreline to the northern half of the deployment area. The southern half of the deployment area contains a 'no-go area' (used for dumping of dredged material) which is excluded from the DTOcean calculation. These domains can also be adjusted to suit the size of deployment being undertaken, as shown in Fig. 3.

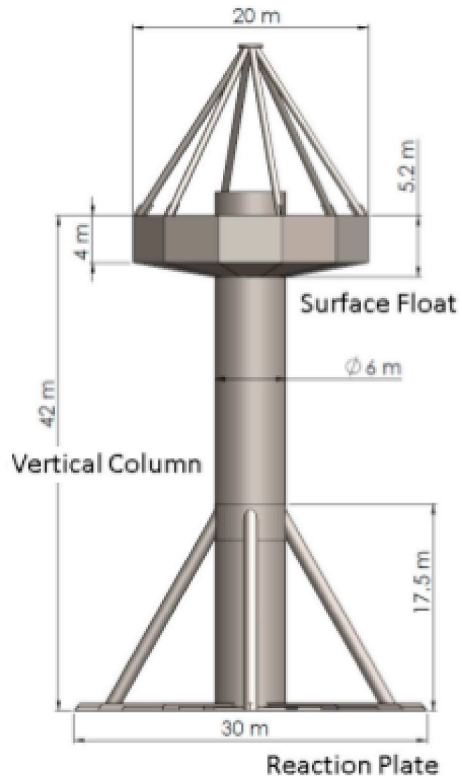

Fig. 7. RM3 device design (from [22], with permission).

The bathymetric and sedimentary data used were acquired from public sources [54,55] and discretised in regular grids, aligned in x and y, using the UTM zone 10N projection. The grid resolution was set to 10m within the deployment area (to allow for accurate cable routing and mooring placement) and 50m within the cable corridor (where less accuracy is required for routing a single cable). The cable corridor slightly overlaps the deployment area to ensure that a subset of grid points is coincident.

The combined seabed depths and sediment are shown in Figs. 4 and 5. Due to limited publicly available data, only a single layer of sediment is defined for the present simulation. This is not anticipated to affect the results as the preferred foundations for the OEC are relatively shallow.

The time series for wave height, period and direction were reused from a pre-existing hindcast model for the site, described in [56], and the resulting occurrence matrix is shown in Fig. 6. This differs slightly from that used in [22], which was derived from an older model. The wind data were obtained from an anemometer on NDBC buoy 46022 and the sea surface currents were collected from an Ocean Surface Current Analyses - Realtime (OSCAR) data point. Although all the data points were not collocated, they do provide a continuous ten year time series (from 2000 to 2009) and are representative of the chosen site.

Extreme environmental values were retrieved from [22,57], NOAA weather station 46022 and the NOAA sea level station at Crescent City, CA.

3.1.2. Ocean energy converter

The floating wave energy converter considered for this study is henceforth known as the 'RM3 device'. As defined in chapter 5 of [22], it is a point wave absorber which can be deployed in water depths between 40m and 100m. The RM3 device design mimics that of the Ocean Power Technology 'PowerBuoy' [58], in that power is generated through the relative motion of a floating buoy reacting against a loosely connected plate, located below the buoy. The arrangement and dimensions are shown in Fig. 7.

The RM3 device generates power from motion in heave and is

H_{m0} [m] \ T_e [s]	4.5	5.5	6.5	7.5	8.5	9.5	10.5	11.5	12.5	13.5	14.5	15.5	16.5	17.5
0.25	0	1	1	1	1	1	1	1	1	1	1	0	0	0
0.75	3	7	9	8	8	11	11	9	8	6	5	4	3	3
1.25	10	18	26	23	23	31	29	25	21	17	14	12	9	8
1.75	19	36	50	46	45	61	56	48	40	33	27	22	18	15
2.25	31	59	83	76	75	101	90	78	65	54	44	36	30	25
2.75	48	88	122	113	112	148	133	114	96	79	65	53	44	36
3.25	62	123	169	158	157	203	182	157	131	109	89	73	60	50
3.75	88	163	224	211	209	265	239	206	172	142	117	96	79	66
4.25	111	208	285	271	268	286	286	260	218	180	148	122	100	83
4.75	137	261	286	286	286	286	286	286	268	222	183	150	124	103
5.25	169	286	286	286	286	286	286	286	286	268	219	181	150	124
5.75	201	286	286	286	286	286	286	286	286	286	261	215	178	148
6.25	237	286	286	286	286	286	286	286	286	286	286	252	208	173
6.75	276	286	286	286	286	286	286	286	286	286	286	286	240	200
7.25	286	286	286	286	286	286	286	286	286	286	286	286	275	228
7.75	286	286	286	286	286	286	286	286	286	286	286	286	286	259
8.25	286	286	286	286	286	286	286	286	286	286	286	286	286	286

Fig. 8. Recomposed RM3 device power matrix.

moored in such a way as to reduce the motion in other modes. Three equally spaced foundations are placed on the seabed 300m from the OEC with matching connectors located 30m above the reaction plate (not shown).

As a consequence of modelling the RM3 device with the direct matrix method, the hydrodynamic performance calculation results in a power matrix which differs slightly from that shown in Tables 5–5 of [22]. After capping the power output at the 286kW rating, the power matrix for the present calculation is seen in Fig. 8. The output voltage of the OEC is chosen as 11kV and, unlike the design in [22], a dedicated umbilical connection to the inter-array cabling is used which connects to the OEC below the moorings.

3.2. Layout and energy production

This section presents the array layout and energy production calculated by the DTOcean software. Following [22], the export cable rating is fixed to 33kV for each deployment size. The OEC and electrical network positions for the 10 OEC deployment are shown in Fig. 9 while Fig. 10 shows the layout for 100 OECs. Notice that the southern corner of the 100 OEC deployment area is empty, as expected, due to the 'no-go' dredge dumping zone defined there.

Using a minimum q-factor setting of 0.9, the mean annual energy production per OEC and capacity factor for the three scenarios are given in Table 3. The level of negative interaction increases marginally when 100 OECs are simulated, with the final q-factor being close to unity in all cases. The annual energy production predicted is similar to that reported in [22], where the OEC rating was chosen to produce a capacity factor of approximately 30%. This is despite the differences in the environmental inputs and power matrix discussed earlier.

The calculated efficiency for the electrical network at each deployment size is given in Table 4. The electrical losses for 10 OECs are

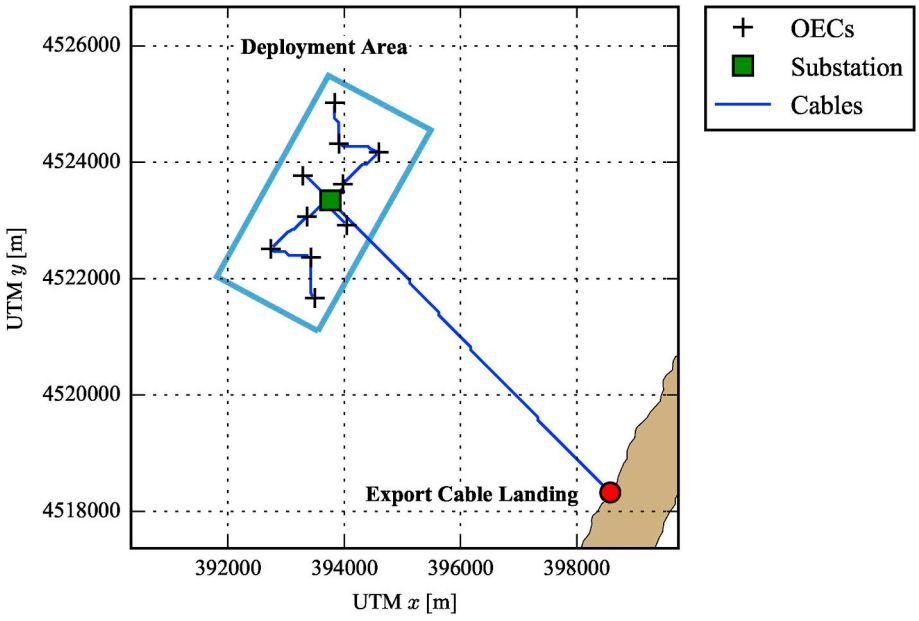

Fig. 9. 10 OEC layout and electrical network.

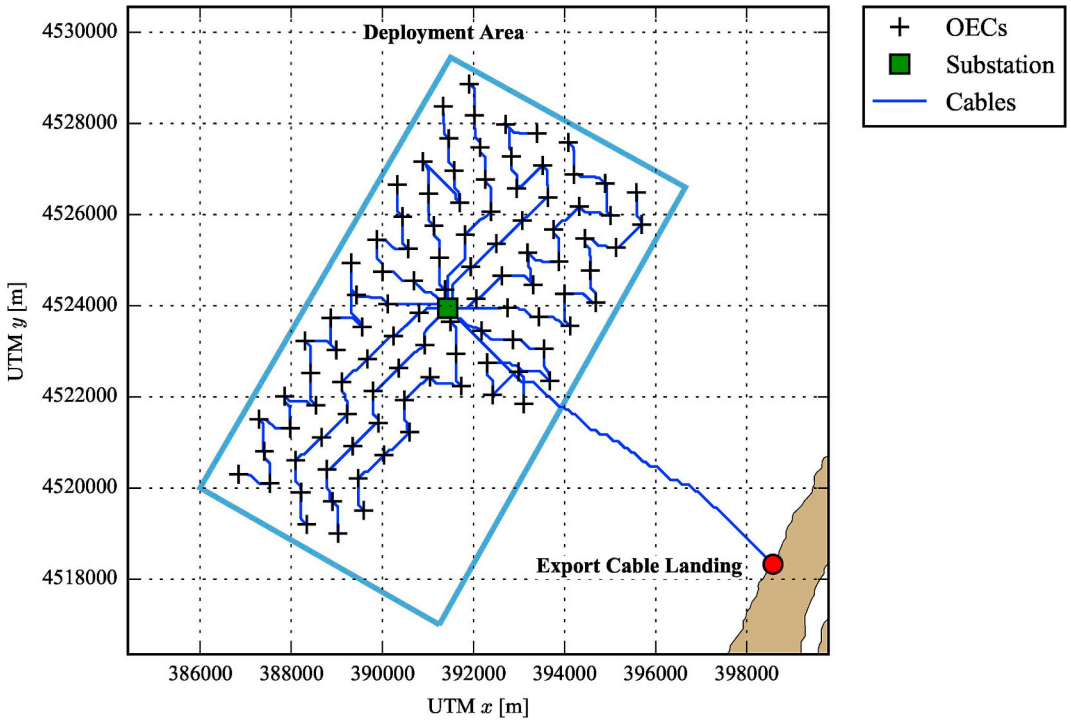

Fig. 10. 100 OEC layout and electrical network.

unusually low, but this is because the 33 kV cable is designed for transmission of significantly higher current than that produced by the 10 OEC array. Accordingly, the electrical losses of this system are negligible. With increasing array size, the transmitted power and number of OECs per branch increases, which reduces the efficiency.

3.3. Component selection and reliability

This section summarises the component selection for the electrical network, moorings and foundations, in terms of costs and reliability. Table 5 presents the cost per rated kW of the components selected. As expected, economies of scale are seen in the electrical sub-systems as more OECs share infrastructure such as the substation and export cable.

The cost per kW for the moorings and foundations of the 50 and 100 OEC deployments are greater than for 10 OECs. Mainly, this is due to installation at greater depths for the 50 and 100 OEC arrays. Also, for the 50 OEC deployment the converters are positioned slightly closer to each other (which makes collision upon line failure more challenging to prevent) resulting in higher costs per kW than the 100 OEC array. Overall, the costs for the 50 and 100 OEC scenarios are similar to that given in [22], which gives a single value for the 10, 50 and 100 OEC deployments. Consequently, the costs for the 10 OEC array are underestimated in comparison.

Drag anchors were set as the preferred foundation type for the simulations as per [22] and the safety factor was calibrated to select an anchor of similar mass to the 9-ton anchor described therein. Notably, for the 50 OEC deployment the sediment type at one foundation was incompatible with drag anchors and thus a gravity foundation was substituted, at higher cost.

The calculated annual failure rates of the external sub-systems for the 50 OEC scenario are shown in Table 6[1] and little variance is seen for the other deployment scales. This is because, due to limited availability of reliability data, a single failure rate per component class is used. Also, DTOcean does not consider the impact of operational factors, such as cable lengths or power transmitted, on failure rates. Thus, any variability in values is a product of the differing number and connectivity of components in a network.

Failures of the OEC's internal sub-systems are simulated with the rates given in Table 7. The failure rate for the power converter is taken from [22]. As no reliability information for the spar buoy or surface float is provided in [22], both are assumed to fail once in 100 years.

3.4. Installation

This section demonstrates the installation planning for the OECs, electrical network and moorings and foundations and serves as an illustration of the logistics algorithms. An arbitrary start date of the 1st of January 2020 was chosen for installation to begin and, following [22], a 10% contingency is applied to the costs. Installation is carried out from the Humbolt Bay deep-water facility.

Table 8 shows the costs per kW installed power, t_{pause} over all operations (T_{pause}) and total installation time for the three deployment sizes. The costs are representative of the $1000/kW price given in [22]

Table 3
Array energy production.

Number of OECs	Annual energy production (MWh)	Capacity factor (%)
10	7380.0	29.46
50	36997.4	29.53
100	71562.7	28.56

Table 4
Electrical network efficiency (%).

Number of OECs	Efficiency
10	100.0
50	97.6
100	93.7

[1] The reliability of the moorings and foundations are calculated together, but maintained as separate sub-systems which results in matching failure rates.

Table 5
Total component costs per rated output (Euro/kW).

Number of OECs	Electrical Sub-Systems	Moorings and Foundations
10	1049	1385
50	420	1746
100	354	1731

Table 6
External sub-system failure rates for the 50 OEC scenario. Parenthesis indicate range of values across all OECs.

Sub-system	Annual failure rate
Export cable	0.079
Substation	0.001
Inter-array cables	(0.114, 0.149)
Umbilical cable	0.131
Moorings	(0.031, 0.163)
Foundations	(0.031, 0.163)

Table 7
Internal sub-system failure rates for the RM3 device.

Sub-system	Annual failure rate
Spar buoy	0.01
Surface float	0.01
Power converter	1

Table 8
Installation operations costs and durations.

Number of OECs	Cost (Euro/kW)	T_{pause} (Hours)	Total time (Days)
10	1148	0	119
50	1278	518	477
100	1394	1947	685

Table 9
Time-based maintenance intervals (years).

Sub-system	Interval
Power converter	1
Umbilical cable	2
Moorings	3
Foundations	3

for the 100 OEC array but the trend with scale differs. Table 8 shows costs increasing with scale whereas [22] reports a 200% reduction between the 10 and 100 OEC arrays.

The increasing value of T_{pause} seen in Table 8 is the key reason for the increasing costs. This is occurring due to the long operation durations required for a single vessel to install the larger arrays (particularly for the umbilical cable phase, which has low OLCs). Another consequence of the long operation durations is that the time to complete the installation increases significantly between the 10 and 100 OEC deployments, from 119 to 685 days. As can be seen in Fig. 11, the challenge of undertaking work in the winter causes delays until the following year. The effect of delays caused by seasonality on the installation is not considered in [22], but it is important as the LCOE calculation involves discounting.

3.5. Lifetime energy and costs

The operational costs, energy production and levelised cost of energy of the scenario is determined. As discussed in section 2.6, these values are subject to variability and thus are presented as statistical distributions and metrics.

The maintenance program described in [22] assumed that two operations per year per OEC were required to service the power converter, umbilical cables, moorings and foundations. For this study, selected sub-systems have been given the time-based maintenance intervals as seen in Table 9. The remaining sub-systems are only serviced upon failure.

Due to the relatively high rate of failure the inter-array cables and lack of time-based maintenance, the vessel mobilisation and preparation time for unplanned corrective maintenance of the sub-system is set

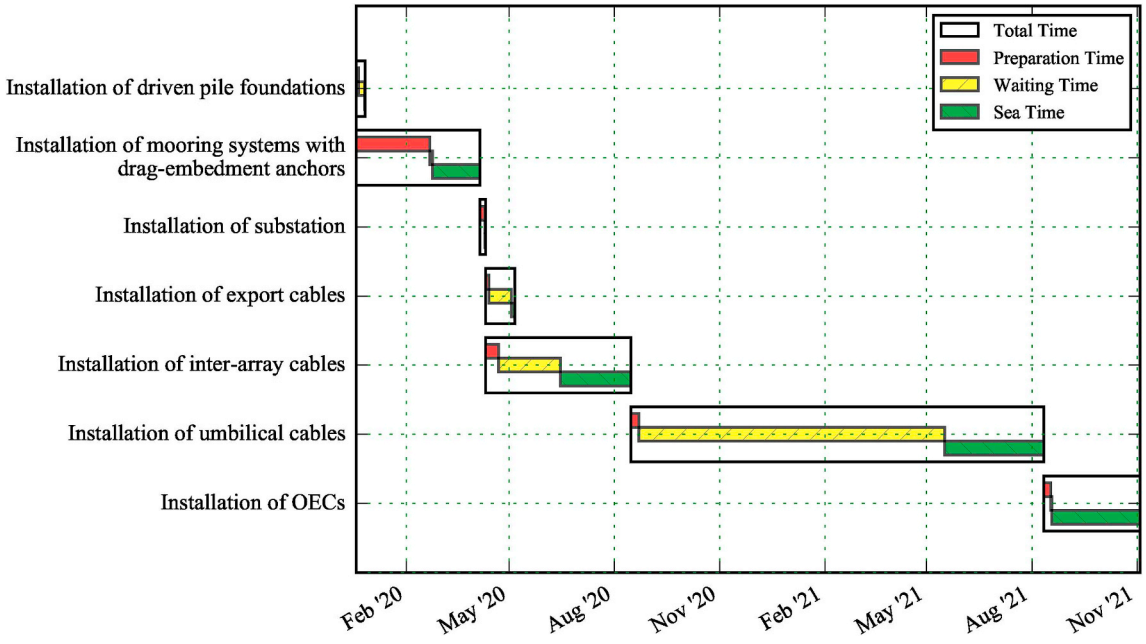

Fig. 11. 100 OEC installation phases Gantt chart.

Table 10
Additional cost inputs, from [22] (millions of Euro).

(a) CAPEX

Number of OECs	Environmental monitoring	Contingency	Total
10	5.71	3.9	9.61
50	7.15	14.9	20.05
100	7.15	30.0	37.15

(b) OPEX

Number of OECs	Environmental monitoring	Insurance	Total
10	2.70	0.81	3.51
50	2.03	1.35	3.38
100	2.03	1.35	3.38

to zero. This avoids cascading failure, due to delays, which can produce unrealistically high amounts of downtime, particularly for the 100 OEC array.

Additional inputs to the CAPEX and OPEX, which are not modelled in DTOcean, contribute to the LCOE calculated in [22]. To improve the comparison, pre-installation environmental monitoring and contingency costs (in addition to the contingency applied to the installation costs) are added to the present study as a one-off CAPEX contribution. Additionally, post-installation environmental monitoring and insurance costs are added annually to the OPEX. The additional costs are shown in Table 10. Following [22], a discount rate of 7% is applied here; additional financial parameters, such as tax rates, are not included.

Thirty samples of the OPEX and AEP histories are collected for each deployment size. The data points, probability density and 95th percentile contour for the 10 and 100 OEC arrays as shown in Figs. 12 and 13. The bivariate correlations are -0.527 and -0.493, respectively. The most likely LCOE and the 95th percentile range (the metric for variability) is given in Table 11 and the breakdown per major contributor to the CAPEX and OPEX is given in Table 12. The most likely LCOE is in general agreement with [22] for each deployment size. A comparison of the probability distributions of the 10 and 100 OEC arrays, normalised by their most likely values, is shown in Fig. 14.

3.6. Impact of investment

As the inter-array cable sub-system is not subject to time-based maintenance, and given that the sub-system failure rate is relatively high, it is prudent to examine the impact on LCOE of investing in higher reliability components.

The sub-system consists of two component types: 11kV static cables and wet-mate connectors. Utilising eq. (7), a linear model of component manufacturing cost with respect to reliability is examined (i.e. $i = 1$ in eq. (7)). The baseline cable cost is 100 Euro/m for an MTTF of 0.2 million hours, so choosing $A = 25$ Euro/m, as the zero reliability cost, implies $B = 375$. This value is reused as the gradient of the wet-mate connector model, having baseline costs of 200 Euro per unit for an MTTF of 0.25 million hours. Therefore, the resulting models are:

$$c_i(\theta_i) = 25 + 375\theta_i$$

$$c_j(\theta_j) = 65 + 375\theta_j$$

where c_i, θ_i and c_j, θ_j are the component cost and reliability (MTTF) of the cable and connector, respectively.

Permutations of three values of each component, shown in Table 13, are tested against the result of the unaltered components for the 10 OEC array given in Table 11. Significance of each LCOE distribution is checked using the energy statistic test with 1000 permutations and a

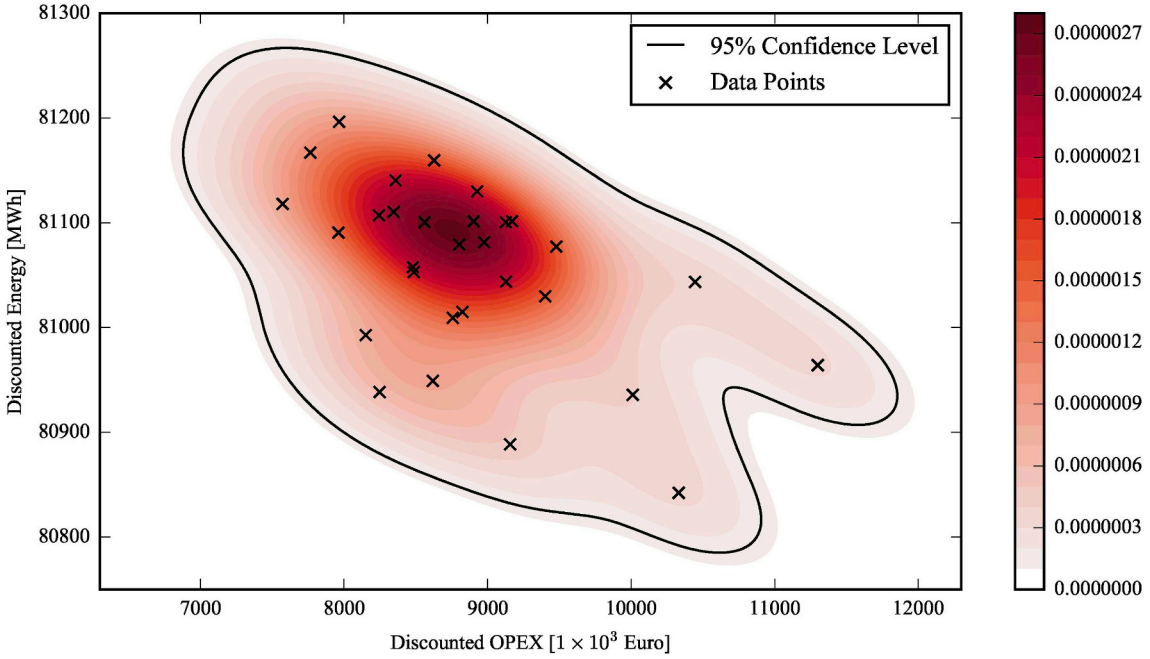

Fig. 12. Bivariate probability density of discounted OPEX and discounted energy for the 10 OEC array. Additional OPEX costs are excluded.

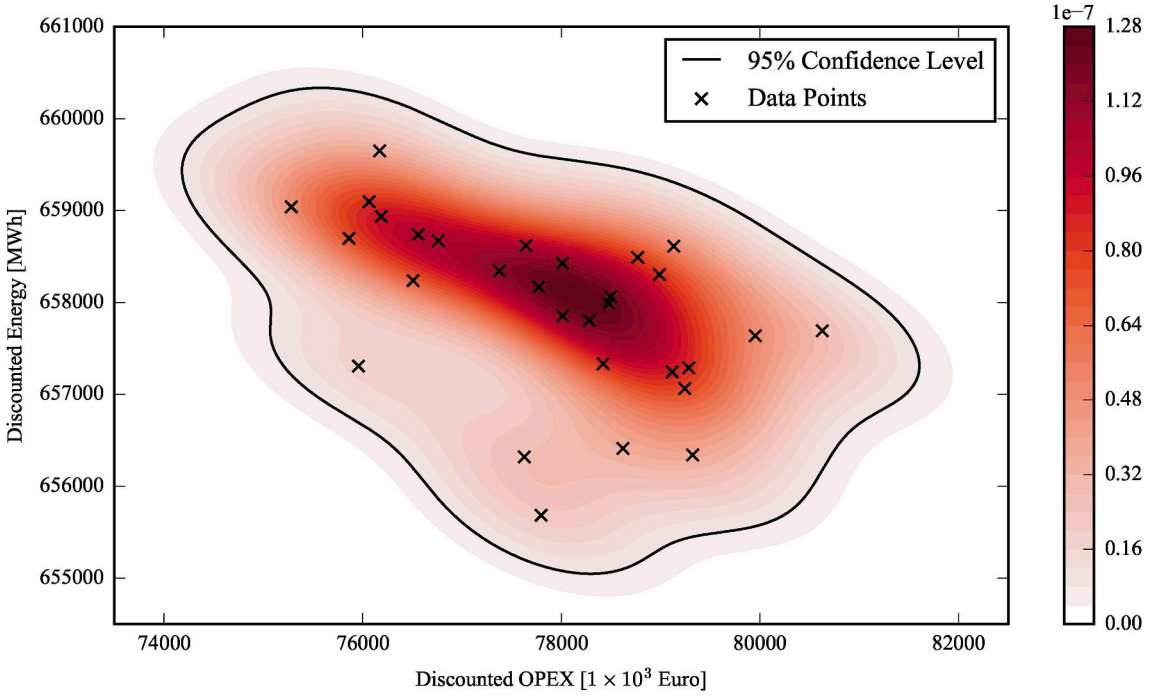

Fig. 13. Bivariate probability density of discounted OPEX and discounted energy for the 100 OEC array. Additional OPEX costs are excluded.

Table 11
Levelised cost of energy (Euro cent/kWh).

Number of OECs	Most likely	95th percentile range
10	110.11	107.68–114.15
50	68.63	67.71–70.42
100	69.06	68.29–69.67

Table 12
Contribution to most likely levelised cost of energy (Euro cent/kWh).

	10 OECs	50 OECs	100 OECs
OECs	24.66	27.08	30.39
Electrical network	3.68	1.62	1.53
Moorings and foundations	4.88	6.71	7.47
Installation	4.05	4.95	6.06
Pre-installation monitoring & contingency	11.85	5.97	5.65
CAPEX total	49.12	46.33	51.1
Operations	14.08	12.18	12.28
Post-installation monitoring & insurance	46.9	10.12	5.68
OPEX total	60.98	22.30	17.96

pass level of $p = 0.05$. The most likely LCOE, 95th percentile range and percentage change to the unaltered case is shown in Table 14. It can be seen that each combination of components produces a significantly different distribution to the base case.

4. Discussion

Through development of the RM3 case study it has been demonstrated that the DTOcean software can simulate a complex OEC array in a detailed and highly integrated manner. Particular points of interest regarding the design, such as the incompatibility of drag anchors at certain regions of the deployment area (section 3.3) and the additional time required to undertake installation due to weather conditions (section 3.4), show the merits of an integrated approach.

Non-parametric bivariate distributions of discounted lifetime energy production and discounted lifetime OPEX (illustrated by Figs. 12 and 13) were used to calculate the most likely LCOE values. As might be anticipated, a negative correlation between the OPEX and AEP is observed, as variation in OPEX is mostly driven by unplanned maintenance events. The most likely LCOE over the three deployment scales (10, 50 and 100 OECs), given in Table 11, was in general agreement with [22], although economies of scale between the 50 and 100 OEC arrays were not observed. This was because the CAPEX component of LCOE (after removing external costs) was shown to increase. Cost savings accrued from sharing electrical infrastructure were offset by increasing costs in the mooring systems and reduced electrical network efficiency, as the size of the arrays increased, as seen in Table 12.

The analysis also provides a measure of variability by calculating the 95th percentile range. It was shown that the variability in the LCOE decreased with deployment scale for the case study herein. Fig. 14 compares the 10 and 100 OEC array probability distributions, normalised by the most likely values. From here, it is clear that the reduction in dispersion of OPEX values, with increasing scale, is the main contributor to the reduction in LCOE variability. This likely occurs because the probability of failures being concentrated into particular seasons is higher for small arrays. Thus, in effect, larger arrays smooth out the differences in maintenance costs caused by seasonal weather variation.

One strategy for reducing the variability found in the LCOE could be to invest in increasing the reliability of the components. Table 14 shows the outcomes from component upgrades for the inter-array cables, assuming a linear manufacturing cost model. Improvements observed in most likely LCOE could be regarded as marginal (up to 2.51%); however, when considering the contribution to CAPEX from the electrical network (7.5% for 10 OECs) they become more relevant. Improvement in variability was more pronounced, reducing by as much as 56.26%. Interestingly, the greatest reduction in variability was observed for different conditions to the greatest reduction in most likely LCOE. It follows that the typical strategy of investing to reduce LCOE may run contrary to the importance of minimising potential cost variance. Further investigation is required to accurately quantify the error in the

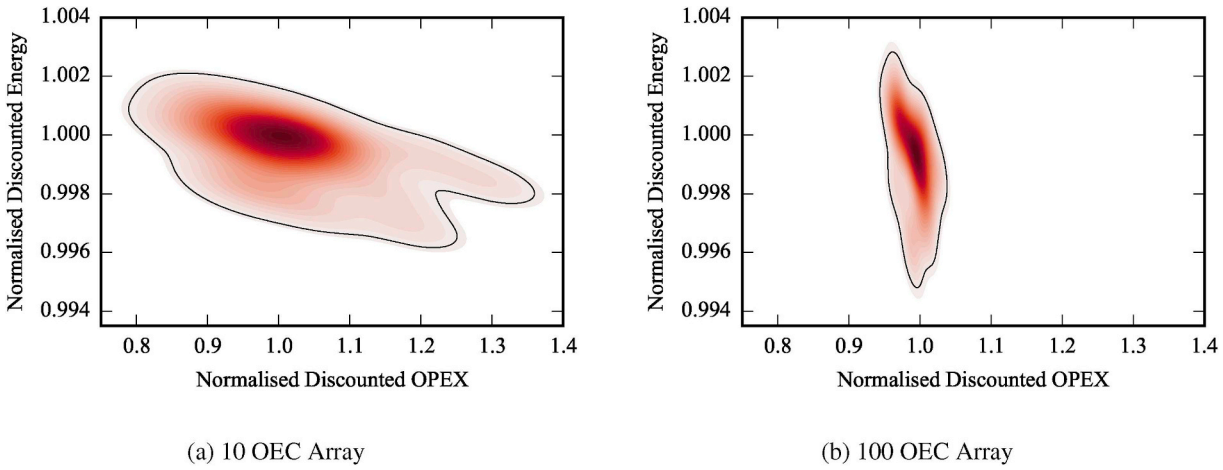

Fig. 14. Bivariate probability distributions of discounted OPEX and discounted energy, normalised by the most likely values.

Table 13
Linear models for manufacturing costs.

(a) 11kV static cables

Index	θ_i (1×10^6 hours)	$c_i(\theta_i)$ (Euro/m)
1	0.2	100
2	0.4	175
3	0.8	325

(b) 11kV wet-mate connectors

Index	θ_i (1×10^6 hours)	$c_i(\theta_i)$ (Euro/m)
1	0.25	200
2	0.5	293.75
3	1	481.25

Table 14
LCOE and 95th percentile range for upgraded static cable and wet-mate connector combinations with comparison to the 10 OEC array result.

#	Static cable	Wet-mate connector	Test p-value	Most likely LCOE (Euro cent/kWh)	Change (%)	95th percentile range (Euro cent/kWh)	Change (%)
1	1	1	–	110.11	–	6.47	–
2	1	2	0.001	108.17	-1.76	4.08	-36.94
3	1	3	0.001	108.24	-1.70	5.36	-17.16
4	2	1	0.001	109.34	-0.70	5.52	-14.68
5	2	2	0.001	108.84	-1.15	3.7	-42.81
6	2	3	0.001	107.35	-2.51	4.45	-31.22
7	3	1	0.006	110.82	0.64	5.18	-19.94
8	3	2	0.001	109.12	-0.90	6.74	4.17
9	3	3	0.001	108.13	-1.80	2.83	-56.26

most likely and 95th percentile metrics, for a given number of data points.

It is important to observe that the results discussed above pertain to a very prescriptive maintenance strategy and are derived from coarse estimates for the cost and reliability of components. Nonetheless, important trends have been revealed which merit investigation of cost variability on a case by case basis. This is especially true if the highest variability is recorded at the smallest deployment scales (the current maturity level of the industry), and a lower than expected return could deter future investment. Mitigation of these risks could be undertaken by investing in more reliable components, but clear understanding of the relationships between production (or research and development) costs and reliability is critical to determining the optimal level of investment.

5. Conclusion

A parametric model of ocean energy converter (OEC) array design and deployment, with higher complexity than previous models, has been demonstrated. The model fully integrates OEC positioning, power calculation, electrical network and station keeping design, installation of the OECs and infrastructure, lifetime maintenance and downtime prediction. Variability in the levelised cost of energy is revealed by modelling random sub-system failures and weather dependent logistics operations. Utilising the model's component level design, a framework for evaluating the impact of investment into more reliable components is proposed.

A case study of a theoretical floating wave energy converter array was developed as a baseline for investigating cost variability and the impact of investment. The variability in levelised cost of energy (LCOE) is shown to reduce with increased size of deployment (the 95th percentile range reduced from 5.9% of the most likely LCOE for the 10 OEC array to 2% for the 100 OEC array), indicating that the least reliable energy cost predictions are associated with smaller arrays. Such results may provide an incentive to accelerate development of larger arrays. Should the performance of small arrays be critical to unlocking additional funding, then this may present a risk to sustained investment. Upgrading the reliability of components can reduce predicted energy

cost (over 2.5%) and variability (over 56%), but the lowest cost solution may not be the least variable.

Further work should examine the effect of alternative maintenance strategies on cost variability and investigate sensitivity to choice of component cost model. The influence of other sources of variability, such as power generation and installation actions, also merits further study. Quantifying the error in the economic metrics and understanding the effects of input uncertainty alongside variability is vital for real world applications.

Acknowledgements

Thanks are given to all members of the DTOcean consortium, without whose efforts this work would not have been possible. Special thanks are also given to Dr. Lucy Cradden for her tireless editing of this manuscript. The research leading to this publication is part of the DTOceanPlus project which has received funding from the European Union's Horizon 2020 research and innovation programme under grant agreement No 785921. Funding was also received from the European Community's Seventh Framework Programme for the DTOcean Project (grant agreement No. 608597). The contribution of Sandia National Laboratories was funded by the U.S. Department of Energy's Water Power Technologies Office. Sandia National Laboratories is a multi-mission laboratory managed and operated by National Technology and Engineering Solutions of Sandia, LLC., a wholly owned subsidiary of Honeywell International, Inc., for the U.S. Department of Energy's National Nuclear Security Administration under contract DE-NA0003525. This paper describes objective technical results and analysis. Any subjective views or opinions that might be expressed in the paper do not necessarily represent the views of the U.S. Department of Energy or the United States Government. The image of the RM3 device, in Fig. 7, was reproduced with the permission of Sandia National Laboratories.

References

[1] Segura E, Morales R, Somolinos J, López A. Techno-economic challenges of tidal energy conversion systems: current status and trends. Renew. Sustain. Energy Rev. 2017;77:536–50.
[2] Lehmann M, Karimpour F, Goudey CA, Jacobson PT, Alam M-R. Ocean wave energy in the United States: current status and future perspectives. Renew. Sustain. Energy Rev. 2017;74:1300–13.
[3] Hemer MA, Manasseh R, McInnes KL, Penesis I, Pitman T. Perspectives on a way forward for ocean renewable energy in Australia. Renew. Energy 2018;127:733–45.
[4] López I, Andreu J, Ceballos S, Martínez de Alegría I, Kortabarria I. Review of wave energy technologies and the necessary power-equipment. Renew. Sustain. Energy Rev. 2013;27:413–34. https://doi.org/10.1016/j.rser.2013.07.009.
[5] Yuce MI, Muratoglu A. Hydrokinetic energy conversion systems: a technology status review. Renew. Sustain. Energy Rev. 2015;43:72–82.
[6] Penalba M, Touzón I, Lopez-Mendia J, Nava V. A numerical study on the hydrodynamic impact of device slenderness and array size in wave energy farms in realistic wave climates. Ocean Eng. 2017;142:224–32. https://doi.org/10.1016/j.oceaneng.2017.06.047.
[7] Myers LE, Bahaj AS. An experimental investigation simulating flow effects in first generation marine current energy converter arrays. Renew. Energy 2012;37(1):28–36. https://doi.org/10.1016/j.renene.2011.03.043.
[8] Child B. WaveFarmer. 2017http://production.presstogo.com/fileroot7/gallery/DNVGL/files/original/22cd4d22f7024619b6ad93e43b6ee9d3.pdf, Accessed date: 11 May 2017.
[9] Parkinson S. TidalFarmer. 2017http://production.presstogo.com/fileroot7/gallery/DNVGL/files/original/2a78191829594b208fe7de68077a2e0e.pdf, Accessed date: 11 May 2017.
[10] Ruehl K, Porter A, Chartrand C, Smith H, Chang G, Roberts J. Development, verification and application of the SNL-SWAN open source wave farm code. Proceedings of the 11th european wave and tidal energy conference, Nantes, France. 2015. p. 8.
[11] Roberts Jesse. SNL-Delft3D-CEC. http://energy.sandia.gov/energy/renewable-energy/water-power/market-acceleration-deployment/snl-delft3d-cec/, Accessed date: 6 July 2018.
[12] Nambiar AJ, Collin AJ, Karatzounis S, Rea J, Whitby B, Jeffrey H, Kiprakis AE. Optimising power transmission options for marine energy converter farms. Int. J. Mar. Energy 2016;15:127–39. https://doi.org/10.1016/j.ijome.2016.04.008.
[13] Sharkey F, Bannon E, Conlon M, Gaughan K. Maximising value of electrical networks for wave energy converter arrays. Int. J. Mar. Energy 2013;1:55–69. https://doi.org/10.1016/j.ijome.2013.06.002.
[14] Harris RE, Johanning L, Wolfram J. Mooring systems for wave energy converters: a review of design issues and choices. 3rd international conference on marine renewable energy. 2004. p. 180–9. Blyth, UK.
[15] Gao Z, Moan T. Mooring system analysis of multiple wave energy converters in a farm configuration. 8th European wave and tidal energy conference (EWTEC). 2009. p. 509–18. Uppsala, Sweden.
[16] Morandeau M, Walker RT, Argall R, Nicholls-Lee RF. Optimisation of marine energy installation operations. Int. J. Mar. Energy 2013;3–4:14–26. https://doi.org/10.1016/j.ijome.2013.11.002.
[17] Ambühl S, Marquis L, Kofoed JP, Dalsgaard Sørensen J. Operation and maintenance strategies for wave energy converters. Proc. Inst. Mech. Eng. O J. Risk Reliab. 2015;229(5):417–41.
[18] Gray A, Dickens B, Bruce T, Ashton I, Johanning L. Reliability and O&M sensitivity analysis as a consequence of site specific characteristics for wave energy converters. Ocean Eng. 2017;141:493–511. https://doi.org/10.1016/j.oceaneng.2017.06.043.
[19] Hasager CB, Madsen PH, Giebel G, Réthoré P-E, Hansen KS, Badger J, Pena Diaz A, Volker P, Badger M, Karagali I, et al. Design tool for offshore wind farm cluster planning. EWEA annual conference and exhibition 2015. European Wind Energy Association (EWEA); 2015.
[20] Halevy A. Why your data won't mix. Queue 2005;3(8):50–8.
[21] McDowell J, Jeffcoate P, Khorasanchi M, Johanning L, Bruce T. First steps toward a multi-parameter optimisation tool for floating tidal platforms–assessment of an LCoE-based site selection methodology. Proceedings of the 12th European wave and tidal energy conference. Ireland: Cork; 2017.
[22] V. S. Neary, M. Previsic, R. A. Jepsen, M. J. Lawson, Y.-H. Yu, A. E. Copping, A. A. Fontaine, K. C. Hallett, D. K. Murray, Methodology for Design and Economic Analysis of Marine Energy Conversion (MEC) Technologies, Tech. Rep. SAND2014-9040, Sandia National Laboratories (Mar. 2014).
[23] Clark CE, Miller A, DuPont B. An analytical cost model for co-located floating wind-wave energy arrays. Renew. Energy 2019;132:885–97.
[24] Sharp C, DuPont B. Wave energy converter array optimization: a genetic algorithm approach and minimum separation distance study. Ocean Eng. 2018;163:148–56.
[25] Teillant B, Costello R, Weber J, Ringwood J. Productivity and economic assessment of wave energy projects through operational simulations. Renew. Energy 2012;48:220–30. https://doi.org/10.1016/j.renene.2012.05.001.
[26] Magagna D, Uihlein A. Ocean energy development in Europe: current status and future perspectives. Int. J. Mar. Energy 2015;11:84–104. https://doi.org/10.1016/j.ijome.2015.05.001.
[27] Previsic M. System level design, performance and costs - Oregon state offshore wave power plant. Tech. Rep. E21 EPRI global–WP–006–OR-rev1. EPRI Global; 2004.
[28] U.S. EPA, Exposure Factors Handbook 2011 Edition (Final Report), Tech. Rep. EPA/600/R-09/052F, U.S. Environmental Protection Agency, Washington, DC (2011).
[29] Martin R, Lazakis I, Barbouchi S, Johanning L. Sensitivity analysis of offshore wind farm operation and maintenance cost and availability. Renew. Energy 2016;85:1226–36. https://doi.org/10.1016/j.renene.2015.07.078.
[30] Allan G, Gilmartin M, McGregor P, Swales K. Levelised costs of wave and tidal energy in the UK: cost competitiveness and the importance of “banded” renewables obligation certificates. Energy Policy 2011;39(1):23–39. https://doi.org/10.1016/j.enpol.2010.08.029.
[31] EU Publications Office. Optimal design tools for ocean energy arrays (DTOcean). https://cordis.europa.eu/project/rcn/110303/, Accessed date: 3 May 2019.
[32] EU Publications Office, Advanced Design Tools for Ocean Energy Systems Innovation, Development and Deployment | H2020. https://cordis.europa.eu/project/rcn/214811_en.html, Accessed 15 July 2018.
[33] Gujarathi G, Ma Y-S. Parametric CAD/CAE integration using a common data model. J. Manuf. Syst. 2011;30(3):118–32. https://doi.org/10.1016/j.jmsy.2011.01.002.
[34] DTOcean Online Manual. https://dtocean.github.io/,Accessed 25 April 2019.
[35] Marine energy - Wave, tidal and other water current converters - Part 2: Design requirements for marine energy systems, Tech. Rep. IEC TS 62600-2:2016, International Electrotechnical Commission (Aug. 2016).
[36] Marine energy - wave, tidal and other water current converters - Part 101: wave energy resource assessment and characterization. Tech. Rep. IEC TS 62600-101:2015. International Electrotechnical Commission; Jun. 2015.
[37] Marine energy - wave, tidal and other water current converters - Part 201: tidal energy resource assessment and characterization. Tech. Rep. IEC TS 62600-201:2015. International Electrotechnical Commission; Apr. 2015.
[38] Ruiz PM, Nava V, Topper MB, Minguela PR, Ferri F, Kofoed JP. Layout optimisation of wave energy converter arrays. Energies 2017;10(9):1262.
[39] Babarit A, Delhommeau G. Theoretical and numerical aspects of the open source BEM solver NEMOH. 11th European wave and tidal energy conference (EWTEC2015). 2015.
[40] McNatt JC, Venugopal V, Forehand D. A novel method for deriving the diffraction transfer matrix and its application to multi-body interactions in water waves. Ocean Eng. 2015;94:173–85.
[41] Katic I, Højstrup J, Jensen NO. A simple model for cluster efficiency. European Wind Energy Association Conference and Exhibition; 1986. p. 407–10.
[42] Bauer J, Lysgaard J. The offshore wind farm array cable layout problem: a planar open vehicle routing problem. J. Oper. Res. Soc. Am. 2015;66(3):360–8. https://doi.org/10.1057/jors.2013.188.
[43] Collin AJ, Nambiar AJ, Bould D, Whitby B, Moonem MA, Schenkman B, Atcitty S, Chainho P, Kiprakis AE. Electrical components for marine renewable energy arrays: a techno-economic review. Energies 2017;10(12):1973. https://doi.org/10.3390/en10121973.
[44] Weller S, Johanning L, Victor L, Karimirad M, Heath J, Eddy J, Jensen R, Roberts J, Banfield S. Deliverable 4.5: mooring and foundation module framework for DTOcean tool Tech. rep. 2015.

[45] Lincoln RW. Learning to trade power. Ph.D. thesis, University of Strathclyde; 2011.
[46] Zimmerman RD, Murillo-Sanchez CE, Thomas RJ. MATPOWER: steady-state operations, planning, and analysis tools for power systems research and education. IEEE Trans. Power Syst. 2011;26(1):12–9. https://doi.org/10.1109/TPWRS.2010.2051168.
[47] Weller SD, Hardwick J, Gomez S, Heath J, Jensen R, Mclean N, Johanning L. Verification of a rapid mooring and foundation design tool. Proc. IME M J. Eng. Marit. Environ. 2018;232(1):116–29. https://doi.org/10.1177/1475090217721064.
[48] DTOcean technical manual, Tech. Rep.. DTOcean Consortium; Oct. 2016.
[49] Teillant B, Chainho P, Vrousos C, Vicente P, Charbonier K, Ybert S, Monbet P, Giebhardt J. Deliverable 5.6: report on logistical model for ocean energy and considerations Tech. Rep. DTO_WP5_ECD_D5.6, DTOcean Consortium Jan. 2016.
[50] Scott DW. Multivariate density estimation: theory, practice, and visualization. John Wiley & Sons; 1992.
[51] Huang H-Z, Liu Z-J, Murthy DNP. Optimal reliability, warranty and price for new products. IIE Trans. 2007;39(8):819–27. https://doi.org/10.1080/07408170601091907.
[52] Rizzo ML, Székely GJ. Energy distance. Wiley Interdiscip. Rev. Comput. Stat. 2016;8(1):27–38. https://doi.org/10.1002/wics.1375.
[53] Billinton R, Zhang W. Cost related reliability evaluation of bulk power systems. Int. J. Electr. Power Energy Syst. 2001;23(2):99–112. https://doi.org/10.1016/S0142-0615(00)00046-6.
[54] NOAA Data Discovery Portal. https://data.noaa.gov/datasetsearch/, Accessed date: 19 July 2018.
[55] U.S. Geological Survey. Science data catalog. https://data.usgs.gov/datacatalog/, Accessed date: 19 July 2018.
[56] A. R. Dallman, V. S. Neary, M. Stephenson, Investigation of spatial variation of sea states offshore of Humboldt Bay, CA using a hindcast model, Tech. Rep. SAND2014-18207, Sandia National Laboratories (Sep. 2014).
[57] Berg JC. Extreme ocean wave conditions for northern California wave energy conversion device Tech. Rep. SAND2011-9304 Sandia National Laboratories; Dec. 2011.
[58] Edwards K, Mekhiche M. Ocean Power Technologies Powerbuoy®: system-level design, development and validation methodology. Proceedings of the 2nd marine energy technology symposium. 2014. Seattle, USA.